11th World Congress on Computational Mechanics (WCCM XI)
5th European Conference on Computational Mechanics (ECCM V)
6th European Conference on Computational Fluid Dynamics (ECFD VI)
E. Oñate, J. Oliver and A. Huerta (Eds)

NONLINEAR COMPUTATIONAL HOMOGENIZATION OF PERFUSED POROUS MEDIA USING THE SENSITIVITY ANALYSIS

EDUARD ROHAN AND VLADIMÍR LUKEŠ

European Centre of Excellence, NTIS New Technologies for Information Society,
Faculty of Applied Sciences, University of West Bohemia,
Univerzitní 8, 30614, Pilsen, Czech Republic
e-mail: rohan@kme.zcu.cz, lukes@kme.zcu.cz

Key words: Porous Media, Homogenization, Sensitivity Analysis, Large Deformation, Coupled Problems, Multi-scale Computing

Abstract. The paper deals with efficient methods for two-scale modelling of nonlinear effects in deforming fluid-staurated porous media. Two alterantive approaches are considered. The first one is based on the upscaling the fluid-structure interaction problem involving linear elastic porous medium and the Newtonean compressible fluid. Using the sensitivity analysis of effective coefficients depending on the geometrical configuration a weakly nonlinear formulation can be introduced to capture influences of the deformation on the material properties. The second approach is based on the updated Lagrangean formulation for the Biot medium whereby the effective poroelastic and permeability parameters are derived and computed using the homogenization. This leads to a coupled two-scale problem which need to be solved at any time step increment.

1 INTRODUCTION

In this paper we consider quasistatic flows in saturated porous media with locally periodic structures. Recently a nonlinear model of the Biot-type poroelasticity was proposed to treat situations when the deformation has a significant influence on the permeability tensor controlling the seepage flow and on the other poroelastic coefficients [8]. Under the small deformation assumption and the first order gradient theory of the continuum, the constitutive laws are considered usually in linearized forms involving material constants independent on the field variables, like deformation, or stress. In this context, our treatment of the material coefficients depending on the stress and deformation state can be viewed as an extension of the first order theory, whereby the linear strain kinematics still holds and the initial domain is taken as the reference. In our approach, the poroelasticity model is derived using the homogenization of the elastic solid skeleton with periodic pores saturated by a weakly compressible static fluid [7], whereby the Darcy flow law is obtained by homogenizing the Stokes flow [2]. Such uncoupled treatment was justified for slow quasistatic processes. To respect dependence of the effective properties on the microstructure deformation, we proposed to use the Taylor expansion w.r.t. the macroscopic variables involved in the global problem. For this, the sensitivity analysis well known from the shape optimization is adopted [9]. The resulting weakly nonlinear formulation, cf. [3], involves the effective poroelasticity and permeability coefficients which are linear functions of the macroscopic response.

Then we consider a fully nonlinear model, based on the correct nonlinear kinematics, which has been derived by homogenization of the incremental Updated Lagrangian Formulation. This model brings about several hurdles related to the numerical implementation, as the configuration changes with deforming microstructure.

In numerical examples we focus on comparing the linear and the quasi-linear model based on linear kinematics. A complete numerical study comprising the nonlinear model based on the updated Lagrangean formulation will be subject of a further publication.

2 LINEAR HOMOGENIZED BIOT CONTINUUM

Assuming slow flows through deforming porous structure and quasistatic loading of the solid phase by external forces, the upscaled medium is described by the Biot-Darcy coupled system of equations. It can be derived by the homogenization of two decoupled problems: 1) deformation of a porous solid saturated by static fluid and 2) Stokes flow through the rigid porous structure.

The porous structure has its characteristic size $L_{\rm mic} = \varepsilon \ell_{\rm mic}$ where $\varepsilon > 0$ is the scale parameter. In the next subsections we present the homogenized model which was obtained by the asymptotic analysis with respect to $\varepsilon \to 0$ for the two problems independently.

2.1 Porous elastic solid saturated by static fluid

We consider the static problem of a deformed elastic porous structure saturated by a fluid under a constant pressure, the pores are assumed to be connected.

The poroelastic medium occupies an open bounded domain $\Omega \subset \mathbb{R}^3$ whereby the following decomposition of Ω into the matrix and channel parts is considered: $\Omega = \Omega_m^\varepsilon \cup \Omega_c^\varepsilon \cup \Gamma^\varepsilon$, $\Omega_m^\varepsilon \cap \Omega_c^\varepsilon = \emptyset$, where $\Gamma^\varepsilon = \overline{\Omega_m^\varepsilon} \cap \overline{\Omega_c^\varepsilon}$ is the interface. Further we denote $\partial_{\rm ext}\Omega_m^\varepsilon = \partial\Omega_m^\varepsilon \setminus \Gamma^\varepsilon$ and similarly $\partial_{\rm ext}\Omega_c^\varepsilon = \partial\Omega_c^\varepsilon \setminus \Gamma^\varepsilon$ the exterior boundaries of Ω_m^ε and Ω_c^ε, respectively. Both Ω_m^ε and Ω_c^ε are connected domains.

The deformation of the solid skeleton is governed by the following boundary value problem where $\boldsymbol{u}^\varepsilon = (u_i^\varepsilon)$ is the displacement field and p^ε is the static fluid pressure:

$$
\begin{aligned}
\nabla \cdot (\mathbb{D}^\varepsilon \boldsymbol{e}(\boldsymbol{u}^\varepsilon)) &= \boldsymbol{f}^\varepsilon \,, \quad \text{in } \Omega_m^\varepsilon \,, \\
\boldsymbol{n}^{[m]} \cdot \mathbb{D}^\varepsilon \boldsymbol{e}(\boldsymbol{u}^\varepsilon) &= \boldsymbol{g}^\varepsilon \,, \quad \text{on } \partial_{\rm ext}\Omega_m^\varepsilon \,, \\
\boldsymbol{n}^{[m]} \cdot \mathbb{D}^\varepsilon \boldsymbol{e}(\boldsymbol{u}^\varepsilon) &= -p^\varepsilon \boldsymbol{n}^{[m]} \,, \quad \text{on } \Gamma^\varepsilon \,,
\end{aligned}
\tag{1}
$$

and

$$\int_{\partial\Omega_c^\varepsilon} \boldsymbol{u}^\varepsilon \cdot \boldsymbol{n}^{[c]} \,\mathrm{dS}_x + \gamma p^\varepsilon |\Omega_c^\varepsilon| = -J^\varepsilon \;, \tag{2}$$

where $\mathbb{D}^\varepsilon$ is the elasticity fourth-order symmetric positive definite tensor of the solid and γ is the fluid compressibility. The applied surface-force and volume-force fields are denoted by $\boldsymbol{g}^\varepsilon$ and $\boldsymbol{f}^\varepsilon$, respectively. The outer unit normal vector of the boundary Ω_m^ε is denoted by $\boldsymbol{n}^{[m]}$.

2.2 Stokes flow through rigid porous structure

The steady flow problem through the channel network constituting domain Ω_c^ε is defined in terms of the flow velocity $\boldsymbol{w}^\varepsilon$ and pressure p which satisfy the following relations:

$$\begin{aligned}
-\eta^\varepsilon \nabla^2 \boldsymbol{w}^\varepsilon + \nabla p^\varepsilon = \boldsymbol{f}^\varepsilon \;, &\quad \text{in } \Omega_c^\varepsilon \;,\\
\nabla \cdot \boldsymbol{w}^\varepsilon = 0 \;, &\quad \text{in } \Omega_c^\varepsilon \;,\\
\boldsymbol{w}^\varepsilon = 0 \;, &\quad \text{on } \Gamma^\varepsilon \;,\\
-p^\varepsilon \boldsymbol{n}^{[c]} + \eta^\varepsilon \boldsymbol{n}^{[c]} \cdot \nabla \boldsymbol{w}^\varepsilon = \boldsymbol{g}^\varepsilon \;, &\quad \text{on } \partial_{\mathrm{ext}}\Omega_c^\varepsilon \;,
\end{aligned} \tag{3}$$

where $\boldsymbol{g}^\varepsilon$ is given on the exterior boundary of the channels. By virtue of the small viscosity ansatz, see [5, 2], we define $\eta^\varepsilon = \varepsilon^2\bar{\eta}$ which decreases with the scale. As discussed e.g. in [6], this viscosity scaling applies when the pores are small, so that the viscous forces dominate in the flow.

2.3 The homogenized Biot – Darcy model

The homogenization methods based on the two scale convergence or the unfolding operator techniques [1] can be applied to describe the limit models arising from asymptotic analyses of the problems (1)-(2) and (3) for $\varepsilon \to 0$, as reported in [8].

The local problems (specified below) related to the homogenized model are defined at the representative unit microscopic cell $Y = \Pi_{i=1}^3]0, \ell_i[\subset \mathbb{R}^3$ which splits into the solid part occupying domain Y_m and the complementary channel part Y_c, thus

$$Y = Y_m \cup Y_c \cup \Gamma_Y \;, \quad Y_c = Y \setminus Y_m \;, \quad \Gamma_Y = \overline{Y_m} \cap \overline{Y_c} \;. \tag{4}$$

If the structure is perfectly periodic, the decomposition of the microstructure and the microstructure parameters are independent of the macroscopic position $x \in \Omega$. Otherwise the local problems must be considered "locally", i.e. for almost any $x \in \Omega$.

The local microsructural response is obtained by solving the following decoupled problems:

- Find $\boldsymbol{\omega}^{ij} \in \mathbf{H}^1_\#(Y_m)$ for any $i, j = 1, 2, 3$ satisfying

$$a_Y^m \left(\boldsymbol{\omega}^{ij} + \boldsymbol{\Pi}^{ij},\, \boldsymbol{v}\right) = 0 \;, \quad \forall \boldsymbol{v} \in \mathbf{H}^1_\#(Y_m) \;. \tag{5}$$

- Find $\boldsymbol{\omega}^P \in \mathbf{H}^1_\#(Y_m)$ satisfying

$$a_Y^m\left(\boldsymbol{\omega}^P,\, \boldsymbol{v}\right) = \fint_{\Gamma_Y} \boldsymbol{v}\cdot\boldsymbol{n}^{[m]}\,\mathrm{dS}_y\;, \quad \forall \boldsymbol{v}\in\mathbf{H}^1_\#(Y_m)\;. \tag{6}$$

- Find $(\boldsymbol{\psi}^i, \pi^i) \in \mathbf{H}^1_\#(Y_c)\times L^2(Y_c)$ for $i = 1,2,3$ such that

$$\begin{aligned} \int_{Y_c} \nabla_y \boldsymbol{\psi}^k : \nabla_y \boldsymbol{v} - \int_{Y_c} \pi^k \nabla\cdot\boldsymbol{v} = \int_{Y_c} v_k \quad \forall \boldsymbol{v}\in\mathbf{H}^1_\#(Y_c)\;, \\ \int_{Y_c} q\nabla_y\cdot\boldsymbol{\psi}^k = 0 \quad \forall q\in L^2(Y_c)\;. \end{aligned} \tag{7}$$

Above $a_Y^m(\boldsymbol{w},\,\boldsymbol{v}) = \fint_{Y_m}(\mathbb{D}\boldsymbol{e}_y(\boldsymbol{w})) : \boldsymbol{e}_y(\boldsymbol{v})$ and $\boldsymbol{\Pi}^{ij} = (\Pi_k^{ij})$, $i,j,k = 1,2,3$ with $\Pi_k^{ij} = y_j\delta_{ik}$. Further $\mathbf{H}^1_\#(Y_m)$ is the Sobolev space $\boldsymbol{W}^{1,2}(Y_m)$ of vector-valued Y-periodic functions (the subscript #). By $\fint_D = |Y|^{-1}\int_D$ with $D\subset\overline{Y}$ we denote the local average, although $|Y| = 1$ can always be chosen.

Using the characteristic responses (5)-(7) obtained at the microscopic scale the effective properties of the deformable porous medium are given by the following expressions:

$$\begin{aligned} A_{ijkl} &= a_Y^m\left(\boldsymbol{\omega}^{ij} + \boldsymbol{\Pi}^{ij},\, \boldsymbol{\omega}^{kl} + \boldsymbol{\Pi}^{kl}\right)\;, \\ C_{ij} &= -\fint_{Y_m} \mathrm{div}_y \boldsymbol{\omega}^{ij} = a_Y^m\left(\boldsymbol{\omega}^P,\, \boldsymbol{\Pi}^{ij}\right)\;, \\ N &= a_Y^m\left(\boldsymbol{\omega}^P,\, \boldsymbol{\omega}^P\right) = \fint_{\Gamma_Y} \boldsymbol{\omega}^P\cdot\boldsymbol{n}\,\mathrm{dS}_y\;, \\ K_{ij} &= \fint_{Y_c} \psi_i^j = \fint_{Y_c} \nabla_y\boldsymbol{\psi}^i : \nabla_y\boldsymbol{\psi}^i\;. \end{aligned} \tag{8}$$

Obviously, the tensors $\mathbb{A} = (A_{ijkl})$, $\boldsymbol{C} = (C_{ij})$ and $\boldsymbol{K} = (K_{ij})$ are symmetric; moreover $\mathbb{A}$ is positive definite and $N > 0$. The hydraulic permeability $\boldsymbol{K}$ is positive semi-definite in general, although it is positive definite whenever the channels intersect all faces of ∂Y and Y_c is connected.

2.4 Coupled flow deformation problem

The Biot–Darcy model of poroelastic media for quasi-static problems is constituted by the following equations involving the homogenized coefficients:

$$\begin{aligned} -\nabla\cdot\boldsymbol{\sigma} &= \boldsymbol{f}^s \qquad \text{in } \Omega\;, \\ \boldsymbol{B} : \boldsymbol{e}(\dot{\boldsymbol{u}}) + M\dot{p} &= -\nabla\cdot\boldsymbol{w} \qquad \text{in } \Omega\;, \\ \boldsymbol{\sigma} &= \mathbb{A}\boldsymbol{e}(\boldsymbol{u}) - \boldsymbol{B}p) \qquad \text{in } \Omega\;, \\ \boldsymbol{w} &= -\frac{\boldsymbol{K}}{\bar{\eta}}\left(\nabla p - \boldsymbol{f}^f\right) \qquad \text{in } \Omega\;, \end{aligned} \tag{9}$$

where $\boldsymbol{B} := \boldsymbol{C} + \phi\boldsymbol{I}$ and $M := N + \phi\gamma$. The volume effective forces acting in the solid and fluid phases are denoted by $\boldsymbol{f}^s$ and $\boldsymbol{f}^f$, respectively.

3 WEAKLY NONLINEAR MODEL

In [8] we established a weakly nonlinear model based on the Biot-Darcy model, assuming a range of small deformations and linear kinematics, so that the linear Cauchy strain is the deformation measure with all its consequences.

3.1 Material perturbation of the effective medium

By $\mathcal{M}(Y)$ we denote a reference microscopic configuration featured by the domain decomposition (4) and by the elasticity $\mathbb{D}(y)$ distributed in Y_m. Let $\tilde{\boldsymbol{u}}(x,y)$ by the "a posteriori" micro-displacement field constituted by the locally homogeneous deformation and by locally periodic fluctuations. Using $\tilde{\boldsymbol{u}}(x,y)$ the initial microscopic configuration can be transformed to a spatial deformed one denoted by $\tilde{\mathcal{M}}(\tilde{\boldsymbol{u}}(x,\cdot),Y)$ and associated with domain $\tilde{Y}(x) = Y + \{\tilde{\boldsymbol{u}}(x,\cdot)\}_{y\in Y}$ for $x \in \Omega$. Due to the sensitivity analysis explained in [8], the perturbed coefficients $H(\tilde{\mathcal{M}}(\tilde{\boldsymbol{u}},Y))$ can be approximated using the first order expansion formulae; in particular

$$
\begin{aligned}
\tilde{H}(\boldsymbol{e}(\boldsymbol{u}),p) &= H^0 + \delta_{\boldsymbol{e}} H^0 : \boldsymbol{e}(\boldsymbol{u}) + \delta_p H^0 p \;, \\
(\delta_{\boldsymbol{e}} H^0)_{ij} &:= \left(\partial_{\boldsymbol{e}}(\delta H^0 \circ \tilde{\boldsymbol{u}})\right)_{ij} = \delta H^0 \circ (\boldsymbol{\omega}^{ij} + \boldsymbol{\Pi}^{ij}) \;, \\
\delta_p H^0 &:= \partial_p(\delta H^0 \circ \tilde{\boldsymbol{u}}) = \delta H^0 \circ (-\boldsymbol{\omega}^P) \;,
\end{aligned}
\tag{10}
$$

where coefficients H^0 are computed using (8) for the reference "initial" configuration $\mathcal{M}(Y)$ and δH^0 are sensitivities w.r.t. the configuration transformations which, in the context of the shape optimization, are given by the so called design velocity fields, cf. [4].

3.2 Problem formulation

Boundary conditions must be prescribed for the displacement and the pressure fields. For this, decomposition of $\partial\Omega$ into disjoint parts is considered:

$$
\partial\Omega = \partial_\sigma\Omega \cup \partial_u\Omega \;, \quad \partial_\sigma\Omega \cap \partial_u\Omega = \emptyset \;, \quad \partial\Omega = \partial_w\Omega \cup \partial_p\Omega \;, \quad \partial_w\Omega \cap \partial_p\Omega = \emptyset \;. \tag{11}
$$

The following conditions are imposed:

$$
\begin{aligned}
\boldsymbol{u} = 0 \;, &\quad \text{on } \partial_u\Omega \;, &\quad \boldsymbol{n}\cdot\boldsymbol{\sigma} = \boldsymbol{g}^s \;, &\quad \text{on } \partial_\sigma\Omega \;, \\
p = p_\partial \;, &\quad \text{on } \partial_p\Omega \;, &\quad \boldsymbol{n}\cdot\boldsymbol{w} = w_n \;, &\quad \text{on } \partial_w\Omega \;.
\end{aligned}
\tag{12}
$$

For the weak formulation the following spaces and admissibility sets are introduced

$$
\begin{aligned}
\boldsymbol{U}(\Omega) &= \{\boldsymbol{u} \in \mathbf{H}^1(\Omega) |\; \boldsymbol{u} = 0 \text{ on } \partial_u\Omega\} \;, \\
P(\Omega) &= \{p \in H^1(\Omega) |\; p = p_\partial \text{ on } \partial_p\Omega\} \;,
\end{aligned}
\tag{13}
$$

whereby the space $P_0(\Omega)$ is defined according to $(13)_2$ with $p_\partial \equiv 0$. Formally we shall use $\boldsymbol{U}_0(\Omega)$ which is identified with $\boldsymbol{U}(\Omega)$ due to (12).

Using the generic form approximation (10) of the perturbed homogenized coefficients we define the nonlinear model by replacing constants $(\mathbb{A}, \boldsymbol{B}, M, \boldsymbol{K})$ employed in (9) by linear extensions depending on the macroscopic response. Thus we get the following system to be satisfied by the couple $(\boldsymbol{u}, p) \in \boldsymbol{U}(\Omega) \times P(\Omega)$

$$
\begin{aligned}
&\int_\Omega \left(\tilde{\mathbb{A}}\boldsymbol{e}(\boldsymbol{u}) - p\tilde{\boldsymbol{B}}\right) : \boldsymbol{e}(\boldsymbol{v}) = \int_\Omega \tilde{\boldsymbol{f}}^s \cdot \boldsymbol{v} + \int_{\partial\Omega} \tilde{\boldsymbol{g}}^s \cdot \boldsymbol{v} \, \mathrm{dS}_x \;, \quad \forall\, \boldsymbol{v} \in \boldsymbol{U}(\Omega) \;, \\
&\int_\Omega q \left(\tilde{\boldsymbol{B}} : \boldsymbol{e}(\dot{\boldsymbol{u}}) + \dot{p}\tilde{M}\right) + \int_\Omega \frac{\tilde{\boldsymbol{K}}}{\bar{\eta}} \left(\nabla_x p - \boldsymbol{f}\right) \cdot \nabla_x q = 0 \quad \forall q \in P_0(\Omega) \;,
\end{aligned}
\tag{14}
$$

where $\tilde{\boldsymbol{f}}^s$ and $\tilde{\boldsymbol{g}}^s$ attain the form (10) due to their dependence on the volume fraction ϕ.

Residual based formulation — sequential linearization Problem (14) is nonlinear because of solution-dependent effective parameters given according to (10). A linearization scheme can be introduced for the time-discretized problem with the time step Δt, so that (14) is transformed in an incremental problem for each time level. The subproblems can be solved in subsequent iterations using updates of the coefficients.

The whole algorithm of computing the state at time level t using the response at time $t - \Delta t$ consists of "solve-and-update" iteration steps which are repeated until the convergence holds: Given $(\boldsymbol{u}^0, p^0) \approx \big(\boldsymbol{u}(t-\Delta t, \cdot), p(t-\Delta t, \cdot)\big)$, compute $(\boldsymbol{u}, p) \approx \big(\boldsymbol{u}(t, \cdot), p(t, \cdot)\big)$, so that $\Psi^t((\boldsymbol{u}, p), (\boldsymbol{v}, q)) = 0$ for any $(\boldsymbol{v}, q) \in \boldsymbol{U}_0(\Omega) \times P_0(\Omega)$, where the residuum of the non-steady formulation is given as

$$
\begin{aligned}
\Psi^t((\boldsymbol{u}, p), (\boldsymbol{v}, q)) = &\int_\Omega \left(\tilde{\mathbb{A}}\boldsymbol{e}(\boldsymbol{u}) - p\tilde{\boldsymbol{B}}\right) : \boldsymbol{e}(\boldsymbol{v}) + \int_\Omega q \left(\tilde{\boldsymbol{B}}\boldsymbol{e}(\boldsymbol{u} - \boldsymbol{u}^0) + \tilde{M}(p - p^0)\right) \\
&+ \frac{\Delta t}{\bar{\eta}} \int_\Omega \tilde{\boldsymbol{K}} \left(\nabla_x p - \boldsymbol{f}\right) \cdot \nabla_x q - \int_\Omega \tilde{\boldsymbol{f}}^s \cdot \boldsymbol{v} - \int_{\partial\Omega} \tilde{\boldsymbol{g}}^s \cdot \boldsymbol{v} \;.
\end{aligned}
\tag{15}
$$

4 EXTENSION FOR LARGE DEFORMATION

The weakly nonlinear model presented in the preceding section is limited in its applicability by the linear kinematics of deformations. When large deformation must be captured it is necessary to resort to the nonlinear continuum mechanics. We propose to use the rate formulation of the balance laws imposed in the actual (deformed) configuration and to use the concept of the updated Lagrangean formulation as the linearization scheme.

4.1 Residual based Eulerian formulation

Let us introduce the following residual which arises from conditions (9) being imposed in the actual deformed configuration:

$$
\begin{aligned}
\Phi_t((\boldsymbol{u},p);(\boldsymbol{v},q)) = & \int_{\Omega(t)} \boldsymbol{\sigma} : \nabla \boldsymbol{v} - \int_{\partial_\sigma \Omega(t)} \boldsymbol{g}^s \cdot \boldsymbol{v} \, \mathrm{dS} \\
& + \int_{\Omega(t)} (\boldsymbol{B} \nabla \dot{\boldsymbol{u}} q + \boldsymbol{K} \nabla p \cdot \nabla q + q M \dot{p}) - \mathcal{J}_t(q) \;,
\end{aligned}
\tag{16}
$$

where $\dot{\boldsymbol{u}}$ is the skeleton (local) velocity, $\mathcal{J}_t(q)$ is the surface source/sink flux enthalpy distribution and the Cauchy stress is given by

$$
\boldsymbol{\sigma} = \boldsymbol{\sigma}^{\mathrm{eff}} - p \boldsymbol{B} = J^{-1} \boldsymbol{F} \boldsymbol{S} \boldsymbol{F}^T \;, \tag{17}
$$

where $\boldsymbol{\sigma}^{\mathrm{eff}}$ is the effective stress associated with the strain energy accumulated in the hyperelastic skeleton, $\boldsymbol{S}$ is the second Piola-Kirchhoff bulk stress, $J = \det \boldsymbol{F}$ and $\boldsymbol{F}$ is the deformation gradient w.r.t. the initial configuration. For simplicity we disregard volume forces. The weak formulation of the force equilibrium and the fluid mass conservation is as follows: Find $\boldsymbol{u}(t,\cdot) \in \boldsymbol{U}(\Omega(t))$ and $p(t,\cdot) \in P(\Omega(t))$ such that

$$
\Phi_t((\boldsymbol{u},p);(\boldsymbol{v},q)) = 0 \quad \forall (\boldsymbol{v},q) \in \boldsymbol{U}(\Omega(t)) \times P_0(\Omega(t)) \;, \tag{18}
$$

where the admissibility sets are defined according to (13).

4.2 Incremental formulation with homogenization feedback

The stress $\boldsymbol{\sigma}^{\mathrm{eff}}$ is a nonlinear function of deformation; its time increment is related to an objective rate. Thus, to solve problem (18), a linearization scheme is needed. Using the Lie derivative and the time differentiation of residual Φ_t w.r.t. a convection field, a rate form of (18) can be obtained. The time discretization $\{t_k\}$ with $t_{k+1} = t_k + \delta t$ leads to the following formulation which allows for computing of the displacement and pressure increments: Find $(\boldsymbol{u},p) \in \delta \boldsymbol{U}(\Omega(t_{k+1})) \times \delta P(\Omega(t_{k+1}))$ which satisfy

$$
\begin{aligned}
& \int_\Omega \mathbb{D}^{\mathrm{eff}} e(\boldsymbol{u}) : e(\boldsymbol{v}) + \int_\Omega \boldsymbol{\sigma}^{\mathrm{eff}} : \nabla \boldsymbol{v} (\nabla \boldsymbol{u})^T - \int_\Omega p [\boldsymbol{B} + \tilde{\boldsymbol{B}}(\boldsymbol{u})] : \nabla \boldsymbol{v} \\
& = \int_\Omega \hat{p} [\boldsymbol{B} + \tilde{\boldsymbol{B}}(\boldsymbol{u})] : \nabla \boldsymbol{v} + \int_\Omega \hat{p} \delta \boldsymbol{B} : \nabla \boldsymbol{v} - \int_\Omega \left(\boldsymbol{\sigma}^k : \nabla \boldsymbol{v} - \rho \boldsymbol{b}^{k+1} \cdot \boldsymbol{v} \right)
\end{aligned}
\tag{19}
$$

for all $\boldsymbol{v} \in \boldsymbol{U}(\Omega(t_k))$ and

$$
\begin{aligned}
& \int_\Omega q [\boldsymbol{B} + \tilde{\boldsymbol{B}}(\bar{\boldsymbol{u}})] : \nabla \boldsymbol{u} + \int_\Omega q (M + \tilde{M}(\bar{\boldsymbol{u}})) p + \delta t \int_\Omega \left(\boldsymbol{K} + \tilde{\boldsymbol{K}}(\bar{\boldsymbol{u}}) \right) \nabla p \cdot \nabla q \\
& = \int_\Omega q \, [\boldsymbol{B} - \delta \boldsymbol{B}] : \nabla \bar{\boldsymbol{u}} + \int_\Omega q (M - \delta M) \bar{p} + \delta t \mathcal{J}^{k+1}(q) - \delta t \int_\Omega (\boldsymbol{K} + \boldsymbol{H}(\bar{\boldsymbol{u}}) + \delta \boldsymbol{K}) \nabla \hat{p} \cdot \nabla q \;,
\end{aligned}
\tag{20}
$$

for all $q \in P_0(\Omega(t_k))$ where

$$
\begin{aligned}
\tilde{\boldsymbol{B}}(\boldsymbol{v}) &= \boldsymbol{B}(\nabla \cdot \boldsymbol{v} - (\nabla \boldsymbol{v})^T) \; , \\
\tilde{\boldsymbol{K}}(\boldsymbol{v}) &= (\nabla \cdot \boldsymbol{v})\boldsymbol{K} - \boldsymbol{K}(\nabla \boldsymbol{v})^T - (\nabla \boldsymbol{v})\boldsymbol{K}^T \; , \\
\tilde{M}(\boldsymbol{v}) &= M \nabla \cdot \boldsymbol{v} \; ,
\end{aligned}
\tag{21}
$$

and the following abbreviated notation is employed with indices k labelling the time levels:

$$
\begin{aligned}
&\delta \boldsymbol{u}^{k+1} \mapsto \boldsymbol{u} \; , \quad \delta \boldsymbol{u}^k \mapsto \bar{\boldsymbol{u}} \; , \quad p^k = \hat{p} \; , \\
&\delta p^{k+1} \mapsto p \; , \quad \delta p^k \mapsto \bar{p} \; .
\end{aligned}
\tag{22}
$$

We recall that poroelastic coefficients $\mathbb{D}^{\text{eff}}, \boldsymbol{B}, M$ and the permeability $\boldsymbol{K}$ are computed using the characteristic responses $\boldsymbol{\omega}^{ij}$, $\boldsymbol{\omega}^P$ and $\boldsymbol{\psi}^i$ defined in (5)-(7), respectively, whereby correspondence $\mathbb{D}^{\text{eff}} = \mathbb{A}$ holds. However, the bilinear form $a_Y^m(\cdot, \cdot)$ is defined in terms of the local incremental tangent modulus of the hyperelastic material for which the strain energy depends on the local "microscopic" displacement field. The local microstructures must be updated after each computed time increment; for this the local characteristic responses and the macroscopic strains and pressure fileds are employed. Coefficients $\delta\boldsymbol{K}, \delta\boldsymbol{B}, \delta M$ are given using sensitivity expressions, see [8] for more details.

5 EXAMPLE

We compare responses of the linear (LB) and weakly nonlinear (WNB) models of the Biot continuum. A column specimen is perfused by *glycerin* ($\gamma = 2.299 \times 10^{-10}$ Pa^{-1}, $\eta = 0.95$ Pa.s) with a pressure difference between the upper and lower surfaces ($p_{in} > p_{out}$), see Fig. 1. The elastic skeleton is made of *polystyrene* ($E = 3.0 \times 10^9$ Pa, $\nu = 0.34$). The scale factor is $\varepsilon_0 = 0.001$ (the size effect of pores related to the fluid viscosity). In Fig. 2 the difference between the LB and WNB models are illustrated using the fluid pressure and strains as functions of the longitudinal position z within the specimen; note the nonlinear distribution of p for the WNB model. Figs. 3-4 reveal the influence of microstructure geometry. Due to the anisotropy of the effective permeability (especially for the 2nd microstructure) there are end-effects apparent in the seepage distributions; these effects are amplified by the nonlinearity, see Fig. 5.

6 CONCLUSIONS AND DISCUSSION

The paper is devoted to extensions of the Biot model of poroelasticity to capture some nonnegligible effects which arise due to the dependence of effective material parameters on the deformation of the microstructure. These parameters are obtained by upscaling the fluid-structure interaction problem using the two-scale homogenization method. We proposed two nonlinear models using two different approaches. The first one (leading to the weakly nonlinear model) uses the framework of the structural sensitivity known from the field of shape optimization, here adapted to obtain expansion formulae for homogenized coefficients, although only linear kinematics is employed. The second is based on

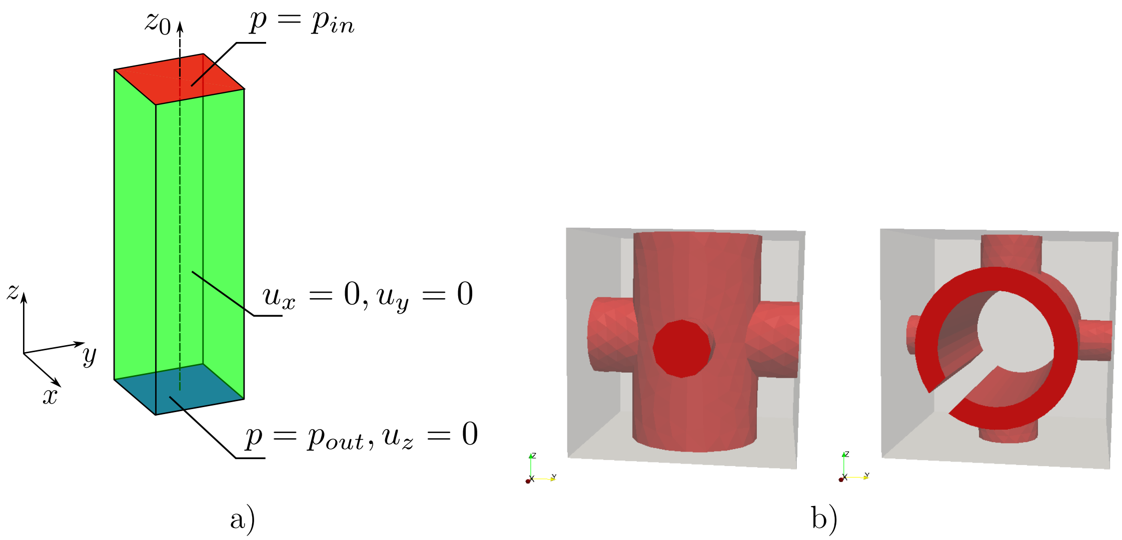

Figure 1: Geometries of the macroscopic domain and representative unit cell: a) macroscopic domain Ω ($0.0167\times0.0167\times0.1$ m) and applied Dirichlet boundary conditions; b) two distinct microscopic geometries Y decomposed into the solid matrix Y_m (transparent gray) and channel part Y_c (red).

the Eulerian rate formulation which leads to an incremental algorithm with simultaneous updating the local microstructures. This second approach is much more expensive from the point of computation, approaching the complexity of "FEM-square" methods. Our further research is focused on development of a more efficient computational algorithm for the fully nonlinear model using the coefficient approximation using sensitivity analysis.

In the numerical example we compared response of the linear and the weakly nonlinear models. We can conclude that the differences in their responses are significant, whereby the most pronounced effects are induced by the deformation-dependent permeability. Both the LB and WNB models are implemented in our in-house code SfePy, see http://sfepy.org.

Acknowledgment This research is supported by project NT 13326 of the Ministry of Health of the Czech Republic, in part by project GACR 13-00863S of the Scientific Foundation of the Czech Republic and by the European Centre of Excellence, CZ.1.05/1.1.00/02.0090.

REFERENCES

[1] Cioranescu, D., Damlamian, A. and Griso, G. The periodic unfolding method in homogenization, *SIAM Journal on Mathematical Analysis* (2008) **40**:1585–1620.

[2] Cioranescu D., Damlamian A., Griso G. The Stokes problem in perforated domains by the periodic unfolding method. New trends in continuum mechanics. *Theta Ser.Adv.Math* (2005) **3**:67–80.

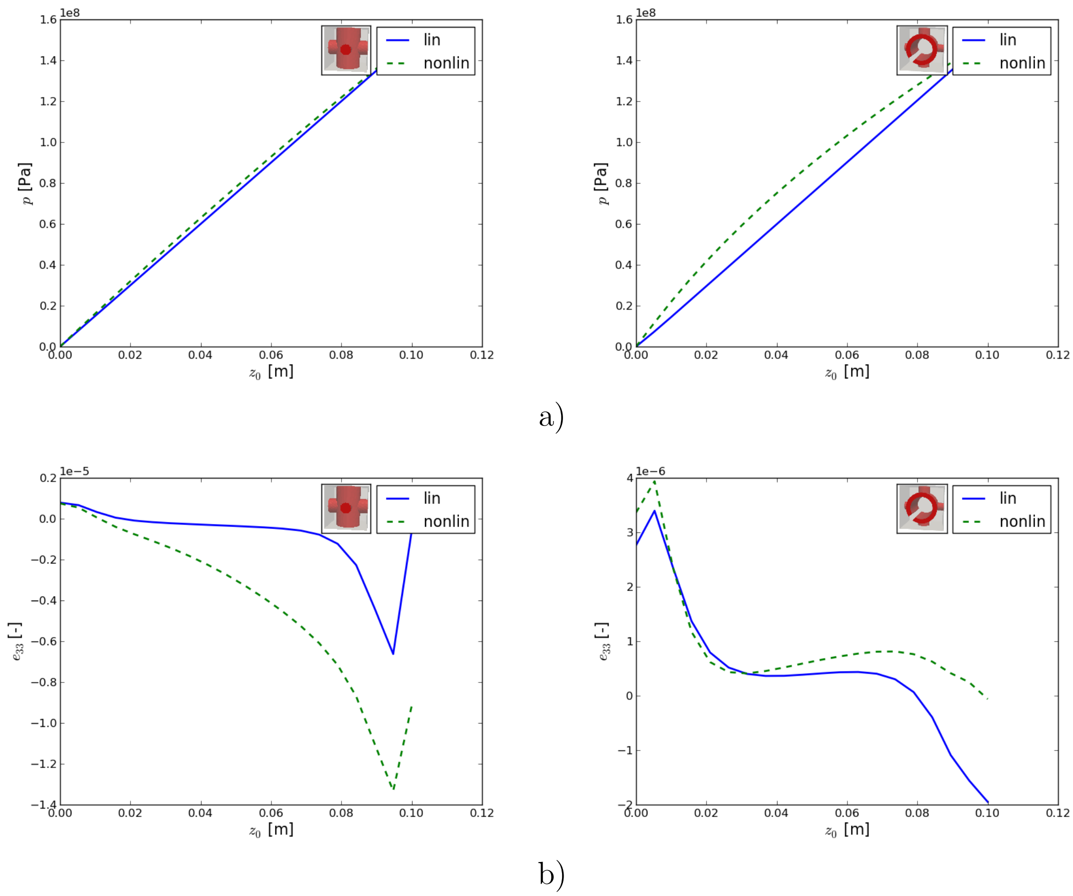

Figure 2: Responses of the linear (LB) and weakly nonlinear (WNB) models along axis z_0, see Fig. 1, depicted for two different microscopic unit cells: a) fluid pressure; b) component e_{33} of the Cauchy strain tensor.

[3] Dormieux, L., Molinari, A. and Kondo, D. Micromechanical approach to the behavior of poroelastic materials. *Jour. Mech. Phys. Solids.* (2002) **50**:2203–2231.

[4] Haslinger, J. and Neittaanmäki, P. *Finite Element Approximation for Optimal Shape, Material and Topology Design*, 2nd ed. J. Wiley & Sons, Chichester, U.K., (1996).

[5] Hornung, U. *Homogenization and porous media.* Springer, Berlin, 1997.

[6] Iliev, O., Mikelic, A., Popov, P. On upscaling certain flows in deformable porous media. *SIAM, Multiscale Model. Simul.* (2008) **7**:93–123.

[7] Rohan, E., Naili, S., Cimrman, R. and Lemaire, T. Hierarchical homogenization of fluid saturated porous solid with multiple porosity scales. *Comptes Rendus Mecanique* (2012) **340**:688–694.

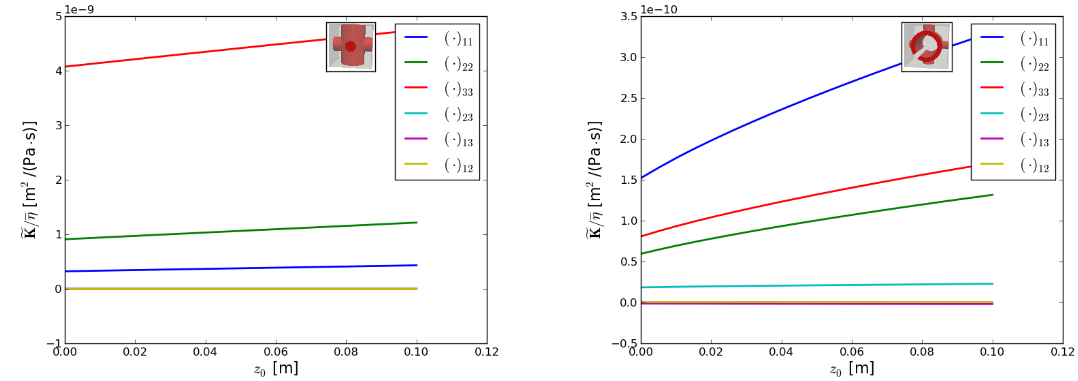

Figure 3: Components of the nonlinear hydraulic permeability tensor $\tilde{K}$ along z_0 axis, $\tilde{K} = \tilde{K}(\boldsymbol{e}(\boldsymbol{u}), p)$.

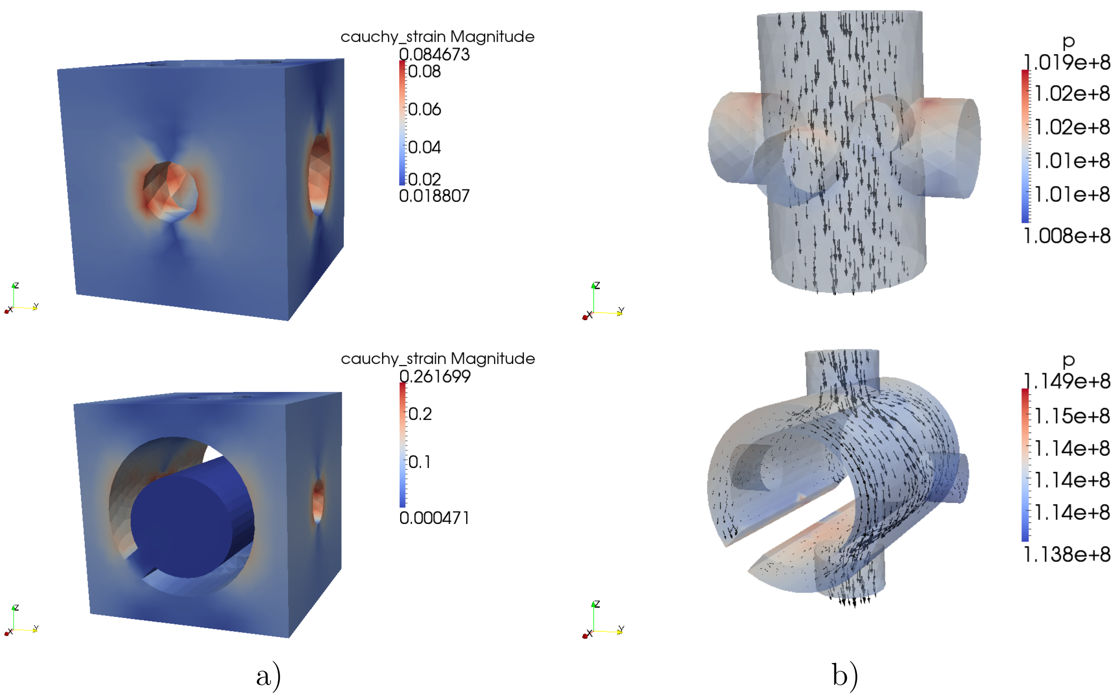

Figure 4: Reconstruction of the strain, pressure and velocity fields at the microscopic level: a) Cauchy strain within the solid part Y_m; b) pressure field and flow velocity in the fluid Y_c.

[8] Rohan, E. and V. Lukeš, V. Modeling flows in periodically heterogeneous porous media with deformation-dependent permeability. Computational homogenization for two-scale modeling of perfused tissues. *Proc. of COMPLAS 2013*, http://congress.cimne.upc.es/complas2013/proceedings/ (2013).

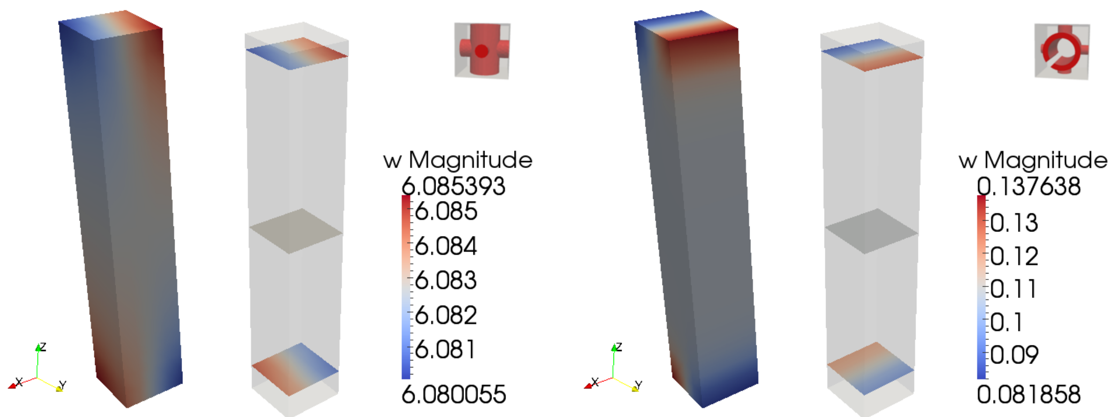

a)

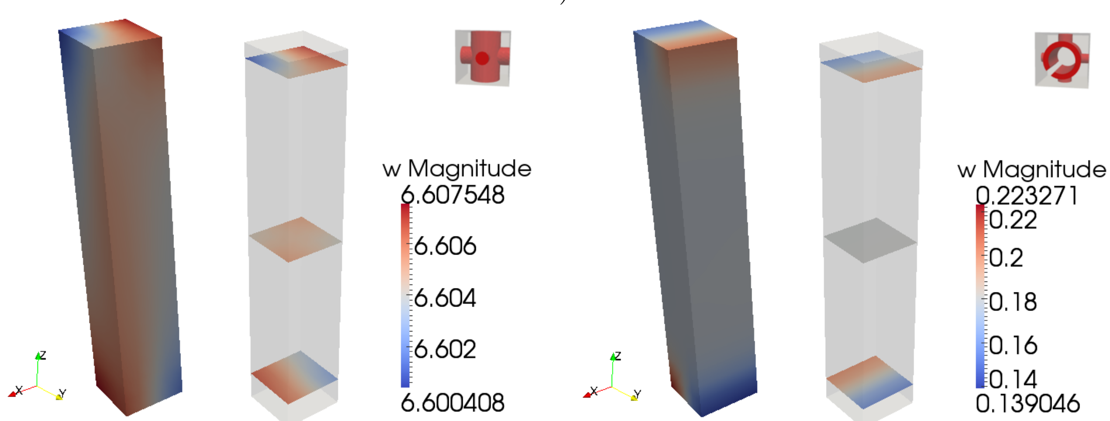

b)

Figure 5: Effect of microstructures, distribution of the seepage velocity in Ω for two distinct underlaying geometries: a) linear model (LB); b) weakly nonlinear model (WNB). Variation of the velocity field in the bar cross-sections is small ($\approx 10^{-3}$) for the 1st microsctructure (left) while more significant differences ($\approx 10^{-1}$) are obtained for the 2nd microstructure (right). ...

[9] Rohan, E. Sensitivity strategies in modelling heterogeneous media undergoing finite deformation. *Math. Comp. Simulation* (2003) **61**:261–270.